Proceedings of the Korean Nuclear Society Spring Meeting
Cheju, Korea, May 1996

Thermal-Hydraulic Aspects of an Advanced Reactor Core with Triangular Lattice Fuel Assemblies

Dae-Hyun Hwang, Yeon-Jong Yoo, Young-Jin Kim, Moon-Hee Chang
Korea Atomic Energy Research Institute

Abstract

Thermal-hydraulic performance has been analyzed for an advanced reactor core loaded with hexagonal fuel assemblies. Currently available CHF prediction models and data base for triangular lattice bundles have been thoroughly reviewed, and as a result the KfK-3 CHF correlation with limit CHFR of 1.235 has been determined to be most appropriate. The pressure drop model in COBRA-IV-I code has been modified for the analysis of triangular lattice rod bundles. In view of maximizing the thermal margin, the geometry of a hexagonal fuel assembly, such as rod diameter and rod pitch, has been optimized with a fixed fuel assembly cross sectional area. The optimum value of the moderator-to-fuel volume ratio is estimated to lie between 0.65 to 1 with 9.5 mm rod diameter. The thermal margin of these hexagonal fuel assemblies in the AP600 core has been evaluated and compared with that of square lattice fuel assemblies such as VANTAGE-5H and KOFA. The analysis result shows that the performances of hexagonal fuel assemblies are more favorable than the square fuel assemblies in the aspect of steady-state overpower margin.

1. Introduction

Hexagonal fuel assembly with triangular-lattice array is a most likely figure to be loaded in the advanced reactor since it has a larger potential for tightening the lattice than the square-lattice array. The potential for tightening the lattice is very important in the aspect of the uranium utilization. The high conversion ratio can be achieved by hardening the neutron spectrum by reducing the moderator-to-fuel volume ratio. Furthermore, it can provide more flexibility to the reactivity control system and consequently contribute to achieving a soluble boron free reactor which will remarkably simplify the reactor system. Due to the circumferential form of the hexagon, it is able to insert more fuel assemblies at a given radius of the core than with the square fuel assemblies. Thus it is possible to achieve lower linear heat rate at the same power level as for the square lattice core. The thermal-hydraulic characteristics of triangular lattice bundles, such as critical heat flux(CHF), pressure drop and interchannel mixing, are quite different from those of square lattice bundles. They are largely influenced by the fuel assembly geometries such as rod diameter, rod pitch, and type of the spacers, and so on. In view of the subchannel geometry, the velocity profile in triangular lattice is much more regular than that in the square lattice, which results in efficient heat removal from the heated surfaces. The hydraulic diameter of triangular lattice channel, however, will be reduced comparing to square lattice channel for the same rod diameter and rod pitch. This may deteriorate the CHF performance and increase the hydraulic resistance in the subchannel. Since existing thermal-hydraulic analysis models for square lattice bundles are mostly not valid for triangular lattice bundles, investigation of adequate thermal-hydraulic models for the analysis of non-square lattice bundle is required in the first place. The CHF and pressure drop prediction models for the triangular lattice bundle have been investigated in this study. The thermal-hydraulic characteristics of triangular lattice bundle have been evaluated in two respects. One is the optimization of a fuel assembly in the aspect of maximizing the thermal margin, and the other is the comparison of the steady-state overpower margins between triangular and square lattice fuel assemblies.

2. Establishment of CHF analysis methodology

Although many CHF correlations have been developed for square lattice rod bundles representing conventional LWRs, most of them are not valid for triangular lattice rod bundles. The applicability of CHF correlations available for the triangular lattice bundles such as the KfK-3[1], PI-3[2], WSC-2[3], and Bowring[4] correlations were investigated. The correlations based on the local parameter hypothesis were not evaluated in this study since they required relevant subchannel analysis codes. CHF data for triangular lattice bundles were collected from open literatures. They are EPRI 19-rod bundle[5], 4 and 7-rod bundles of JAERI[6], and 5x4 triangular lattice bundles by Bettis Atomic Power Laboratory[7]. The major specifications of the test bundles are given in table 1. The prediction accuracies of CHF correlations for triangular array rod bundles were compared in table 2. For the data base considered in this study, KfK-3 CHF correlation shows the best prediction capability among the four correlations. The predicted CHF values by KfK-3 correlation are compared with the measured values in figure 1. The mean error and the standard deviation of P/M for the collected data base were calculated to be 1.9% and 12.2%, respectively. The normality of the P/M distribution was checked by the D'-test[8]. As the result, the correlation limit CHFR was determined to be 1.235 using the Owen's one-sided tolerance factor[9].

3. Subchannel analysis of CHF test bundles

According to the work by Rehme[10] for the pressure drop performance of rod bundles in hexagonal arrangement, the upper limit for the pressure loss coefficients was given by the equivalent annular zone model. For the calculation of subchannel velocity distribution in the triangular lattice bundles, this model was coded into the COBRA-IV-I subchannel analysis code[11]. In the single channel approach the mass velocity of the hot channel (a central coolant channel) was determined on the basis of the hydraulic diameters. Assuming uniform water density, constant friction factors, and equal pressure drop in the various coolant channels, the velocity distribution factor is given by[1]

$$F_G = \frac{G}{G_{avg}} = \frac{(nA + n_w A_w + n_c A_c)\sqrt{D_h}}{nA\sqrt{D_h} + n_w A_w \sqrt{D_{hw}} + n_c A_c \sqrt{D_{hc}}}. \qquad (2)$$

The mass velocity and quality distributions in various test bundles were analyzed by the modified COBRA-IV-I subchannel code, and compared with the results by the single channel approach. The differences between the single channel and the subchannel analyses are attributed to the combined effects due to the test section wall, two-phase pressure drop multiplier, and radial power distributions. In single-phase flow conditions, the velocity distribution factors calculated by the single channel approach are very close to those by the subchannel analysis. In two-phase flow conditions, however, the mass velocity in the hot channel by a subchannel code reduces remarkably by the effect of two-phase pressure drop multipliers. Thus in view of the mass velocity, the subchannel approach is more conservative than the single channel approach. On the other hand, the local quality is largely affected by the radial power distribution. In the 19-rod bundle which had a relatively flat power distribution, turbulent mixing was not effectively occurred by the subchannel analysis since the enthalpy in the hot subchannel is similar to those in the surrounding channels. Consequently the local quality in this case was higher than that by the single channel approach as shown in figure 2. In the 7-rod bundle cases, however, the peak to average power ratios are relatively large, thus the hot channel enthalpy was significantly reduced due to the turbulent mixing between subchannels.

4. Optimization of hexagonal fuel assembly geometry

The geometry of a fuel assembly, such as rod diameter and rod pitch, was optimized in the aspect of maximizing the thermal margin in this study. Considering an equivalent core size to the AP600's[12], the CHFR and bundle pressure drop were calculated for various moderator-to-fuel volume ratio(V_M/V_F) as shown in figure 3. In the low V_M/V_F region, the CHFR decreases due to the effect of decreased hydraulic diameter. On the contrary the CHFR decreases because of the increased local heat flux and decreased mass velocity in the high V_M/V_F region. Consequently the optimum geometry lies approximately between 0.65 to 1.0 of V_M/V_F. The bundle pressure drop of those cases were calculated to be about 0.7 to 1.4 bar which was compatible with the pressure drop for square lattice fuel assembly with IFM grids. For a fixed V_M/V_F, larger thermal margin can be achieved by loading more fuel rods in one assembly. The optimization criterion for this case may be fuel fabrication cost. Based on the results so far achieved, two types of fuel assemblies were selected as the optimum geometry; one is a 331-rod assembly with 9.5 mm rod diameter and 12.6 mm rod pitch and the other is a 397-rod assembly with 9.5 mm diameter and 11.5 mm rod pitch.

5. Evaluation and comparison of thermal margin

Steady-state thermal margin of AP600 core by replacing the existing square lattice fuel assemblies by the hexagonal fuel assemblies were evaluated. The overpower margins for various core inlet temperature conditions were determined on the basis of the CHF design criterion only. The square lattice fuel assemblies considered for the AP600 core were the VANTAGE-5H(V5H) fuel assembly and the KOFA. In the evaluation of thermal margin for V5H core and KOFA core, the COBRA/K110[13] and the TORC/KRB-1[14] CHF analysis system were applied, respectively. The main thermal-hydraulic design parameters used in the thermal margin evaluations are given in table 3. As shown in figure 4, the overpower margin of V5H core was about 17% higher than that of KOFA core. This increase can be readily explained by the effect of turbulence mixing between subchannels which was augmented due to the mixing vanes and IFM grids. Also it is shown that the overpower margin decreases almost linearly as core inlet temperature increases. For the two types of hexagonal fuel assemblies which were chosen from the optimization study, the overpower margins were calculated using the KfK-3 CHF correlation with the limit CHFR of 1.235. It turns out that the overpower margin for 331-rod hexagonal fuel assembly is compatible with that of V5H core as shown in figure 4. The increase of thermal margin for 397-rod hexagonal fuel assembly is attributed to the beneficial effects of increased mass velocity and reduced average heat flux, which offset the thermal margin degradation owing to the reduction of hydraulic diameter.

6. Conclusions

The thermal-hydraulic characteristics of an advanced reactor core loaded with hexagonal fuel assemblies have been evaluated in this study. Main conclusions obtained are as follows:

1) The KfK-3 CHF correlation appears to be most appropriate for the analysis of triangular lattice bundle, which results from the evaluation of CHF data base so far collected with the single channel approach.
2) The optimum value of V_M/V_F to obtain maximum thermal margin lies between 0.65 and 1 for a hexagonal fuel assembly with rod diameter of 9.5 mm.
3) The performance of hexagonal fuel assembly is more favorable than the square fuel assembly in the aspect of steady-state overpower margin.

References

[1] Donne M.D., CHF-KfK-3: A Critical Heat Flux Correlation for Triangular Arrays of Rods with Tight Lattices, KfK-4826 (1991)
[2] Pernica R., Cizek J., PI Correlations for Prediction of Critical Heat Flux in LWR Fuel Assemblies, NURETH-5 paper 2B2 (1992)
[3] Bowring R.W., WSC-2: A Subchannel Dryout Correlation for Water-Cooled Clusters over the Pressure Range 3.4-15.9 MPa, AEEW-R983 (1979)
[4] Bowring R.W., A New Mixed Flow Cluster Dryout Correlation for Pressures in the Range 0.6-15.5 MN/m^2 (90-2250 psia) for Use in a Transient Blowdown Code, IMechE, 175-182 (1977)
[5] Fighetti C.F., Reddy D.G., Parametric study of CHF data, Volume 3: Critical heat flux data, EPRI-NP-2609 3 (1982)
[6] Iwamura T., et al., Critical Heat Flux Experiments for High Conversion Light Water Reactor (Japanese), JAERI-M-90-044 (1990)
[7] LeTourneau B.W., et al., Critical heat flux and pressure drop tests with parallel upflow of high pressure water in bundles of 0.25 and 0.28 inch diameter rods (LWBR development of program), WAPD-TM-1013 (1975)
[8] ANS, Assessment of the assumption of normality(employing individual observed values), ANSI N15.15, (1974).
[9] Owen D.B., Factors for one-sided tolerance limits and for variables sampling plans, SCR-607 (1963).
[10] Rehme K., Pressure Drop Performance of Rod Bundles in Hexagonal Arrangements, Int. J. Heat Mass Transfer 15, 2499-2517 (1972)
[11] Wheeler C.L., et al., COBRA-IV-I: An Interim Version of COBRA for thermal-hydraulic Analysis of Rod Bundle Nuclear Fuel Element and Cores, BNWL-1962 (1976)
[12] Westinghouse Electric Corporation, AP600 Standard Safety Analysis Report, (1992)
[13] 황대현, 신형로 노심 임계열유속 해석체제 개발, RN1-711-004-P Rev.0 (1993)
[14] Hwang D.H., et al., Evaluation of the Thermal Margin in a KOFA-loaded Core by a Multichannel Analysis Methodology, J. KNS 27, 518-531 (1995)

Table 1. Characteristics data for various CHF test bundles

Parameters	EPRI	JAERI B	JAERI C	JAERI D	WAPD
Lattice type	triangular	triangular	triangular	triangular	triangular
Number of heated rods	19	7	7	4	20
Spacer type	grid	grid	grid	grid	grid
Rod diameter, mm	10.72	9.5	9.5	9.5	6.35 - 7.11
Rod pitch, mm	15.14	11.4	10.7	11.4	8.64
Heated length, mm	1524	1000	500	500	1372
Radial peaking factor	1.091	1.281	1.18	1.0	1.0 - 1.5
Axial power profile	uniform	uniform	uniform	uniform	uniform
Pressure, bar	103.4	11 - 39	11 - 39	37 - 39	28 - 138
Mass velocity, $kg/m^2/s$	1348 - 4078	1012 - 2669	1023 - 3087	1162 - 4267	1294 - 5466
Number of data	12	69	58	32	300

Table 2. Statistic of P/M for various CHF correlations

Data base (Number of data)	CHF correlations based on the system parameters							
	KfK-3		PI-3		Bowring		WSC-2	
	Mean	Standard Deviation	Mean	Standard Deviation	Mean	Standard Deviation	Mean	Standard Deviation
EPRI 19-rod (12)	1.189	0.1100	1.103	0.1062	0.942	0.0875	1.467	0.0795
JAERI 7-rod B (69)	1.034	0.1149	0.878	0.0968	1.087	0.0931	1.348	0.0941
JAERI 7-rod C (58)	0.999	0.1087	0.836	0.1383	0.995	0.1215	1.173	0.0979
JAERI 4-rod D (32)	0.857	0.0493	0.809	0.0309	0.662	0.1295	1.054	0.0617
WAPD 20-rod (300)	1.030	0.1157	0.956	0.1146	1.177	0.2369	1.093	0.1405
All data (471)	1.019	0.1224	0.924	0.1265	1.101	0.2428	1.147	0.1626

Table 3. Thermal-hydraulic parameters for the comparison of thermal margins

Parameters	17x17 square fuel assembly	Hexagonal fuel assembly 331-rod	Hexagonal fuel assembly 397-rod
Core thermal power, MWth	1933		
System pressure, bar	155.1		
Core inlet temperature, °C	276.9		
Core flow rate, kg/s	8404.1		
Number of fuel assemblies	145		
Enthalpy rise hot channel factor	1.65		
Axial power profile	1.55 chopped cosine		
Mass velocity, $kg/m^2/s$	2349.7	2543.2	3200.1
Average linear heat rate, kW/m	13.48	12.15	10.12
Average heat flux, kW/m^2	451.1	407.1	339.2
Core pressure drop, bar	1.2	0.74	1.41
Rod diameter, mm	9.5	9.5	9.5
Rod pitch, mm	12.6	12.6	11.5
Number of fuel rods/assembly	264	300	360
Number of guide tubes/assembly	25	31	37
Number of IFM grids	5	0	0

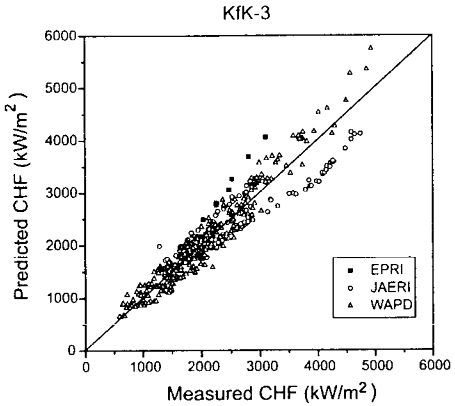

Figure 1. Comparison of predicted CHF values by KfK-3 correlation with measured CHFs.

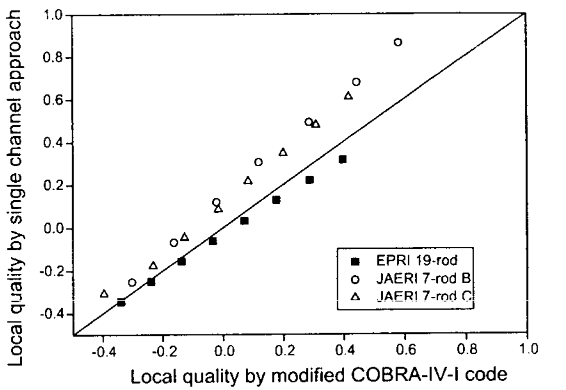

Figure 2. Comparison of local qualities between single channel and subchannel analyses.

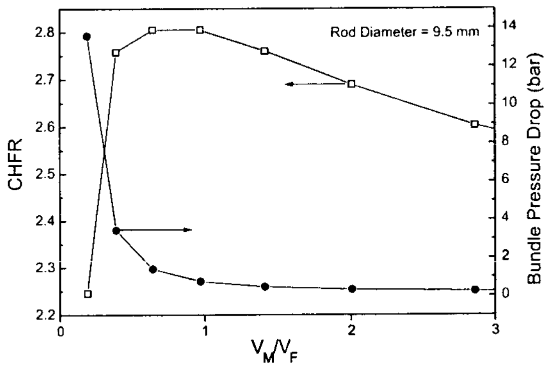

Figure 3. Variation of CHFR and bundle pressure drop for various moderator-to-fuel volume ratios.

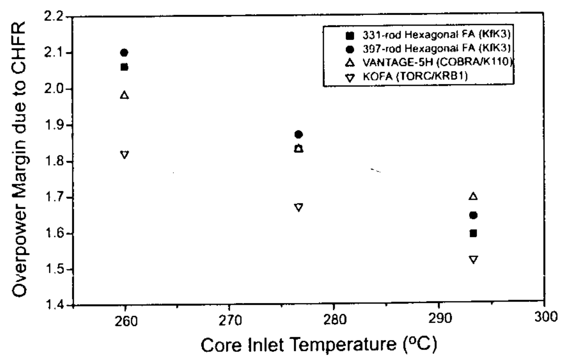

Figure 4. Comparison of overpower margins with various fuel assemblies.